Electronic Supplementary Material (ESI) for ChemComm.
This journal is © The Royal Society of Chemistry 2015

A Switch-On MRI Contrast Agent for Noninvasive Visualization of Methylmercury

Gyan Singh, Kuang-Mei Hsu, Yu-Jen Chen, Shou-Cheng Wu, Chiao-Yun Chen,* Yun-Ming Wang*

Experimental Section

Materials and instrumentations:

4,7,10-(Tris-tert-butylcarboxymethyl)-(1,4,7,10-tetraazacyclodecane) (DO3A-tris-*tert*-butyl ester),[1] compound **1**[2], and **1a**[2] were synthesized following the previously reported procedure with minor modification. Tetra-*n*-butylammonium bromide (TBAB), anhydrous sodium sulfate (Na_2SO_4), 1,3-dibromopropane, 1,2-dibromoethane, boron trifluoride diethyl etherate($BF_3{\cdot}O(C_2H_5)_2$), iron(III) chloride hexahydrate ($FeCl_3{\cdot}6H_2O$), magnesium chloride ($MgCl_2$), zinc bromide ($ZnBr_2$), copper(II) chloride ($CuCl_2$), chloroform-*d*, DMSO-d_6, D_2O, and HEPES were purchased from Sigma-Aldrich. 4-Hydroxybenzaldehyde, 2-hydroxybenzaldehyde, 1,4-dioxane, methyl thioglycolate, and anhydrous potassium carbonate (K_2CO_3) were purchased from Alfa Aesar. 1,4,7,10-Tetraazacyclododecane, sodium chloride (NaCl), and calcium chloride ($CaCl_2$) were purchased from Strem chemicals, J. T baker, and SHOWA, respectively. Potassium chloride (KCl), Mercury(II) chloride ($HgCl_2$), and Methylmercury(II) chloride(CH_3HgCl) were purchased from Merck. All commercial grade chemicals were used without further purification. Luminescence was measured by using a Hitachi F-7000 fluorescence spectrophotometer. ^1H (300 MHz) and ^{13}C (75 MHz) NMR spectra were recorded on a Bruker-300 NMR Spectrometer. The concentration of the Gd(III) complex was determined by ICP-MS(Agilent 7500ce ICP-MS). The relaxivity measurements were performed using a relaxometer operating at 20 MHz and 37.0 ± 0.1 °C (NMR-120 Minispec, Bruker, Germany). MR imaging was performed with a 3.0 T MR scanner (Sigma; GE Medical Systems, Milwaukee, WI) and Bruker 7.0 T MR imaging system (Ettlingen, Germany). The HPLC experiments were performed on an Amersham ÄKTA basic 10 instrument equipped with an Amersham UV-900 detector and Amersham Frac-920 fraction collector. Mass spectral analyses were performed with a Waters Q-Tof (Waters, Milford, Massachusetts).

1. Synthesis

Tri-*tert*-butyl 2,2',2''-(10-(3-(2-formylphenoxy)propyl)-1,4,7,10-tetraazacyclododecane-1,4,7-triyl)triacetate (2)

To the acetonitrile (MeCN) solution (20 mL) of DO3A-tris-*tert*-butyl ester (5.1 g, 10 mmol), were added anhydrous potassium carbonate (K_2CO_3) (6.9 g, 50 mmol) and compound **1** (3.8 g, 14 mmol). The resulting mixture was refluxed for 2 days. The reaction was cooled to room temperature and filtered. The filtrate was evaporated under reduced pressure to leave a yellow gum. The crude product was dissolved in dichloromethane (CH_2Cl_2) and purified on a silica gel column. The mixture was first eluted with ethyl acetate (EtOAc) and then the product was eluted with 5% CH_3OH / CH_2Cl_2. The product was obtained as a white foam in 63% yield (4.3 g, 6.3 mmol). ^{1}H NMR (300 MHz, $CDCl_3$ w/TMS): δ 10.38 (s, 1H), 7.77 (m, 1H), 7.50 (m, 1H),7.00 (m, 2H), 3.67 (brs, 2H), 3.35−2.18 (a set of very broad and multiple peaks with an integration corresponding to 24H), 1.99 (brs, 2H), 1.41-1.38 (m, 27H); ^{13}C NMR (75 MHz, $CDCl_3$ w/TMS): δ 189.47, 189.39, 173.71, 172.74, 170.41, 170.03, 161.13, 160.51, 136.22, 129.45, 128.46, 124.72, 121.03, 120.91, 112.94, 112.63, 82.94, 82.60, 81.85, 67.16, 65.90, 56.93, 56.62, 55.83, 52.78, 50.37, 48.03, 28.12, 27.95, 27.84, 25.94, 23.35; HRESI-MS(ESI$^+$): calculated for $[C_{36}H_{60}N_4O_8]^+$ 676.4411, found 677.4499. The appropriate isotope pattern was observed.

Tri-*tert*-butyl 2,2',2''-(10-(3-(2-(3,9-dioxo-2,10-dioxa-5,7-dithiaundecan-6 -yl) phenoxy) propyl)-1,4,7,10-tetraazacyclododecane-1,4,7-triyl)triacetate (3)

To a solution of **2** (3 g, 4.4 mmol) and methyl thioglycolate (0.72 ml, 13 mmol) in dry CH_2Cl_2 (90 ml), $BF_3{\cdot}Et_2O$ (0.3 ml, 3 mmol) was added slowly. The mixture was allowed to stir at 4 ^{o}C for 12 hrs. After 12 hrs, the reaction was quenched by addition of water (50 ml). The mixture was extracted with CH_2Cl_2 (40 ml×3). The combined organic phase was washed with brine, dried over anhydrous sodium sulfate (Na_2SO_4) and concentrated under reduced pressure. The crude product was dissolved in CH_2Cl_2 and purified on a silica gel column, eluting with 3% CH_3OH in CH_2Cl_2. The product was obtained as a yellowish foam in 76% yield (2.9 g, 3.3 mmol). ^{1}H NMR (300 MHz, $CDCl_3$ w/TMS): δ 7.45 (d, 1H), 6.93 (m, 3H), 5.71(s, 1H), 4.19(brs, 2H), 3.66 (m, 6H), 3.37−2.33 (a set of very broad and multiple peaks with an integration corresponding to 28H), 2.29

(brs, 2H), 1.45-1.43 (m, 27H). ^{13}C NMR (75 MHz, $CDCl_3$ w/TMS): δ 173.80, 172.82, 170.74, 170.53,170.23, 155.40, 155.28, 129.86, 129.63, 128.84, 128.51, 126.84, 126.59, 121.08, 120.87, 82.87, 82.54, 81.81, 66.91, 65.48, 55.67, 55.77, 55.32, 52.62, 49.98, 47.95, 47.67, 47.53, 33.93, 33.79, 33.69, 28.21, 27.92, 25.93, 23.29; HRESI-MS(ESI$^+$): calculated for $[C_{42}H_{70}N_4O_{11}S_2]^+$ 870.4483, found 871.4573. The appropriate isotope pattern was observed.

2,2',2''-(10-(3-(2-(Bis((carboxymethyl)thio)methyl)phenoxy)propyl)-1,4,7,10-tetraazacyclododecane-1,4,7-triyl)triacetic acid (4)

Compound **3** (2.4 g, 2.7 mmol) was dissolved in the mixture (15 mL) of dioxane and sodium hydroxide (NaOH) with the ratio of 3:1 (v/v). This solution was stirred vigorously for about 10 hrs under N_2 at 50 °C. The mixture was concentrated under reduced pressure and the solide obtained was re-dissolved in 60 mL HCl (6N) and allowed to stir at room temprature for next 12 hrs. HCl was removed by coevaporation with water (3 × 100 mL). This compound was purified by AG 1 × 8 anion exchange resin column (200−400 mesh, HCO^{2-} form, eluted first with H_2O and then with a gradient of formic acid. The final product **4** was obtained as a white solide in 29% yield. (0.6 g, 0.8 mmol). ^{1}H NMR (300 MHz, D_20): δ 7.48 (d, 1H), 7.31 (m, 1H), 7.01(m, 2H), 5.38 (s, 1H), 4.08 (m, 2H), 3.26 (m, 4H), 2.97 (brs, 6H), 2.64−2.17 (a set of very broad and multiple peaks with an integration corresponding to 18H), 1.93 (brs, 2H). ^{13}C NMR (75 MHz, D_2O): δ180.31, 179.94, 177.03, 155.11, 129.67, 128.43, 127.68, 120.93, 113.16, 67.65, 59.03, 58.44, 50.90, 50.32, 50.01, 48.90, 47.67, 37.62, 25.06; HRESI-MS (ESI$^+$): calculated for $[C_{28}H_{42}N_4O_{11}S_2]^+$ 674.2291, found 675.2361. The appropriate isotope pattern was observed.

Scheme S1. Synthesis of *p*-MeHgGad

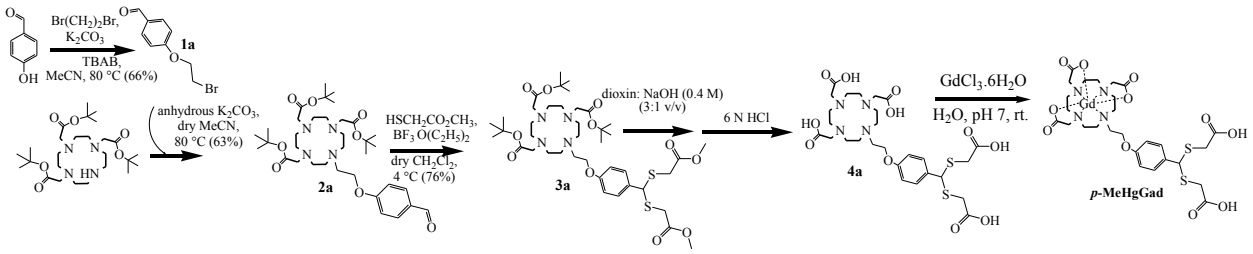

Tri-*tert*-butyl 2,2',2''-(10-(2-(4-formylphenoxy)ethyl)-1,4,7,10-tetraazacyclododecane-1,4,7-triyl)triacetate (2a)

Synthesis procedure is similar to that of compound **2**. ^{1}H NMR (300 MHz, $CDCl_3$ w/TMS): δ 9.84 (s, 1H), 7.73 (d, 2H), 7.19 (d, 2H), 4.33 (brs, 2H), 3.52−2.16 (a set of very broad and multiple peaks with an integration corresponding to 24H), 1.48 (s, 9H), 1.22 (brs, 18H); ^{13}C NMR (75 MHz, $CDCl_3$ w/TMS): δ 191.06, 172.97, 172.67, 163.87, 131.93, 130.61, 115.94, 82.55, 82.41, 65.78, 55.67, 55.88, 52.30, 50.06, 31.14, 28.18, 27.91; HRESI-MS(ESI$^+$): calculated for $[C_{35}H_{58}N_4O_8]^+$ 662.4255, found 663.4321. The appropriate isotope pattern was observed.

Tri-*tert*-butyl 2,2',2''-(10-(2-(4-(3,9-dioxo-2,10-dioxa-5,7-dithiaundecan-6-yl)phenoxy)ethyl) -1,4,7,10-tetraazacyclododecane-1,4,7-triyl)triacetate (3a)

Synthesis procedure is similar to that of compound **3**. ^{1}H NMR (300 MHz, $CDCl_3$ w/TMS): δ 7.29 (d, 2H), 6.96 (d, 2H), 5.24(s, 1H), 4.16 (brs, 2H), 3.71 (s, 6H), 3.50−2.38 (a set of very broad and multiple peaks with an integration corresponding to 28H), 1.46 (m, 9H), 1.26 (brs, 18H). ^{13}C NMR (75 MHz, $CDCl_3$ w/TMS): δ 172.97, 172.64, 170.60, 158.89, 131.19, 129.08, 115.58, 114.93, 82.48, 82.38, 82.14, 65.42, 56.49, 55.81, 53.20, 52.66, 52.34, 50.44, 49.82, 33.91, 31.13, 28.16, 28.01; HRESI-MS(ESI$^+$): calculated for $[C_{41}H_{68}N_4O_{11}S_2]^+$ 856.4326, found 857.4413. The appropriate isotope pattern was observed.

2,2',2''-(10-(2-(4-(Bis((carboxymethyl)thio)methyl)phenoxy)ethyl)-1,4,7,10-tetraazacyclododecane-1,4,7-triyl)triacetic acid (4a)

Synthesis procedure is similar to that of compound **4**. ^{1}H NMR (300 MHz, D_20): δ 7.42 (d, 2H), 6.99 (d, 2H), 5.16 (s, 1H), 4.35 (brs, 2H), 3.75−3.24 (a set of very broad and multiple peaks with an integration corresponding to 28H). ^{13}C NMR (75 MHz, D_2O): δ 174.57, 174.45, 157.56, 131.15, 129.29, 114.81, 52.27, 52.52, 51.65, 49.75, 35.13, 34.92; HRESI-MS (ESI$^+$): calculated for $[C_{27}H_{40}N_4O_{11}S_2]^+$ 660.2135, found 661.2209. The appropriate isotope pattern was observed.

1. Preparation of *o*-MeHgGad

The Gd(III) complex were prepared by dissolving the ligand 4 (0.5 g, 0.74 mmol) in H_2O (10 mL). The pH of the solution was adjusted to 6.5 with dilute sodium hydroxide. A solution of $GdCl_3$ (0.56 g, 0.78 mmol) in 5 mL (pH = 6.5) was added drop wise, maintaining pH at 5.5–6.5 with dilute sodium hydroxide. The mixture solution was stirred at room temperature for 12 hrs and the pH of the solution was periodically monitored and maintained. After 12 hrs the pH of the mixture solution was brought to 8.0, and the solution was centrifuged to remove excess lanthanide ions as $Gd(OH)_3$ and verified by the xylenol orange test. The trace $Gd(OH)_3$ was further removed by filtrating with 200 nm nylon filter, and the solution was freeze-dried under reduced pressure. *o*-MeHgGad was purified by HPLC and identified by HRESI-MS (Fig. S24). Similar procedure were followed for synthesis of *o*-MeHgEura (Eu(III) analog of *o*-MeHgGad) (HRESI-MS spectrum, Fig. S25), *p*-MeHgGad (HRESI-MS spectrum, Fig. S26), and *p*-MeHgEur (Eu(III) analog of *p*-MeHgGad) (HRESI-MS spectrum, Fig. S27, ESI)

Luminescence lifetime measurements

Luminescence measurements were performed on solutions consisting of 500 μM Eu(III) analogues of *o*-MeHgGad in H_2O and D_2O in the absence and presence of CH_3Hg^+. The rate of luminescence decay was measured using a Hitachi F-7000 fluorimeter (San Francisco, CA) with an excitation wavelength of 394 nm and an emission wavelength of 615 nm. The emission lifetimes (τ) values obtained in H_2O and D_2O are is summarized in Table S1. The number of bound water molecules was determined using equations S1 and S2.[3]

$$q = 1.05[1/\tau_{H2O} - 1/\tau_{D2O}] \quad \text{(S1)}$$

$$q = 1.05[(1/\tau_{H2O} - 1/\tau_{D2O}) - 0.25] \quad \text{(S2)}$$

where q is the number of water molecules bound to metal ions, τ_{H2O} is the luminescence half-life in water solution and τ_{D2O} is the luminescence half-life in deuterium oxide solution, respectively.

Table S1 Luminescence lifetimes (ms) and calculated number of inner-sphere water molecules (q) for the Eu (III) analog of *o*-MeHgGad in the absence and presence of CH_3Hg^+

	τ^{-1}_{H2O}	τ^{-1}_{D2O}	q	
			eq 2	*eq 3*
o-MeHgEur[a]	2.207	1.990	0.227	-0.039
o-MeHgEur + 2 equiv. CH_3Hg^+	2.481	0.641	1.932	1.908
p-MeHgEur[b]	2.178	0.519	1.741	1.690

[a]Eu (III) analog of *o*-MeHgGad
[b]Eu (III) analog of *p*-MeHgGad

2. Relaxation time measurement (r_1)

The longitudinal relaxation times (T_1) of Gd(III) complex were measured to determine relaxivity (r_1). All measurements were performed in 20mM HEPES buffer (pH 7.4) using a relaxometer operating at 20 MHz and 37.0 ± 0.1 °C (NMR-120 minispec, Bruker). Before each measurement the relaxometer was tuned and calibrated. The values of r_1 were determined from 5 data points generated by an inversion–recovery pulse sequence. Gd(III) concentrations were determined using ICP-OES. Relaxivity profile of DOTAREM®, *o*-MeHgGad, and *p*-MeHgGad were computed from the slope of the plot of $1/T_1$ vs. [Gd]. Methyl mercury response was determined by the addition of CH_3HgCl dissolved in DMSO (final solutions with Gd contain <5% DMSO by volume) to solutions of the contrast agent. Hg^{2+} response was determined by the addition of $HgCl_2$ dissolved in H_2O. For metal ion selectivity experiments, aqueous NaCl, KCl, $MgCl_2$, $CaCl_2$, $FeCl_3$•$6H_2O$, $CuCl_2$, and $ZnCl_2$ were used.

3. MR imaging study

MR imaging experiment was performed with a 3.0 T MR imaging scanner (Sigma, GE Medical Systems, Milwaukee, WI) using a knee coil. The T_1-weighted scanning was performed under the following condition: fast gradient echo, TR = 200 ms, TE = 61.3 ms, coronal view, and section thickness = mm, FOV = 10 cm.

4. *In vivo* MR imaging study

C57BL/6JNarl mice were purchased from the National Laboratory Animal Center, Taipei, Taiwan. Animal experiments were performed in accordance with our institutional guidelines for animal research. To simulate methyl mercury exposer 100 μL of methylmercury chloride solution (HEPES buffer containing DMSO (2%, v/v)) at the dose of 0.1 mmol/kg was injected intravenously via a tail vein into mice (n = 3). For control experiment three mice were given HEPES buffer injection. After 7 hrs, a single dose of *o*-MeHgGad (0.1 mmol/kg) was administered to each mouse by intravenous injection via the tail vein. The whole-body imaging of pentobarbital-anesthetized mice was performed with a 7.0 T MR imaging system (Bruker, Ettlingen, Germany). MR images were acquired before 4hrs, and 30 minutes after the contrast agent administration using a T_1-weighted fast spin-echo sequence 7.0 T imaging (TR/TE/ flip angle = 400/15/10°) for every 3 mm sectioning thickness. Contrast enhancement were calculated in the regions of interest (ROI) manually drawn on kidney, liver, and intestine using equation S3 and the data is represented as mean ± SD (n = 3)

$$Enhancement\ (\%) = \left[\frac{(SI_{post} - SI_{pre})}{SI_{pre}}\right] \times 100 \qquad \text{(S3)}$$

where SI_{post} and SI_{pre} are the MR signal intesnity determined in the ROI at postcontrast and precontrast, respectively.

Table S2 MR signal enhancement percentage in liver, intestine, and kidney

	-CH_3Hg^+		+ CH_3Hg^+	
	ROI	Enhancement (%)	ROI	Enhancement
Liver	ROI 1	+1.1± 0.1 %	ROI 8	+5.2±0.6%
	ROI 2	+1.3±0.1 %	ROI 9	+20.5±2.7%
Intestine	ROI 3	+0.2±0.4 %	ROI 10	+23.8±4.3%
	ROI 4	+6.9±0.3 %	ROI 11	+18.4±2.7%
	ROI 5	+3.8±0.2 %	ROI 12	+24.7±2.1%
Kidney	ROI 6	+4.4±0.5 %	ROI 13	+18.8±1.2%
	ROI 7	+4.7±1.1 %	ROI 14	+11.5±3.6 %

Table S3 Tissue distributions of Gd(III) and Hg(II) ions 45minutes post intravenous injection of *o*-MeHgGad at the dose of 0.1 mmol/kg in mice treated and not treated with CH_3Hg^+

	Element contents (μg/g)			
	-CH_3Hg^+		+CH_3Hg^+	
	Gd	Hg	Gd	Hg
kidney	23.62	0.063	20.80	10.40
liver	13.88	0.088	16.40	5.76
intestine	12.15	0.042	12.70	3.55

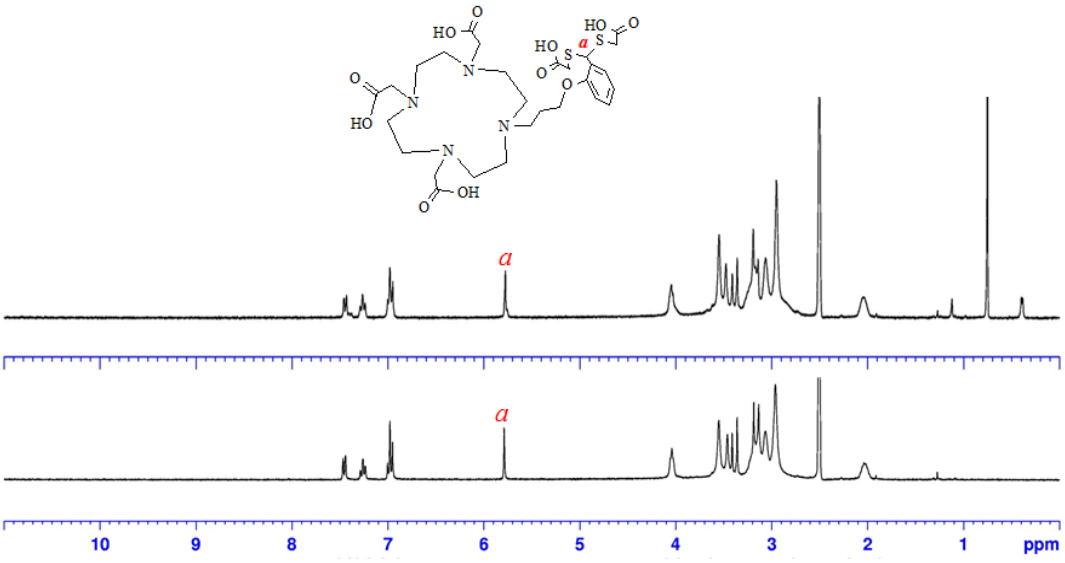

Fig. S1 ^{1}H NMR spectra (dry DMSO-d_6, 300 MHz): (A) *o*-MeHgGad ligand; (B) 1:3 mixture of *o*-MeHgGad ligand and CH_3Hg^+.

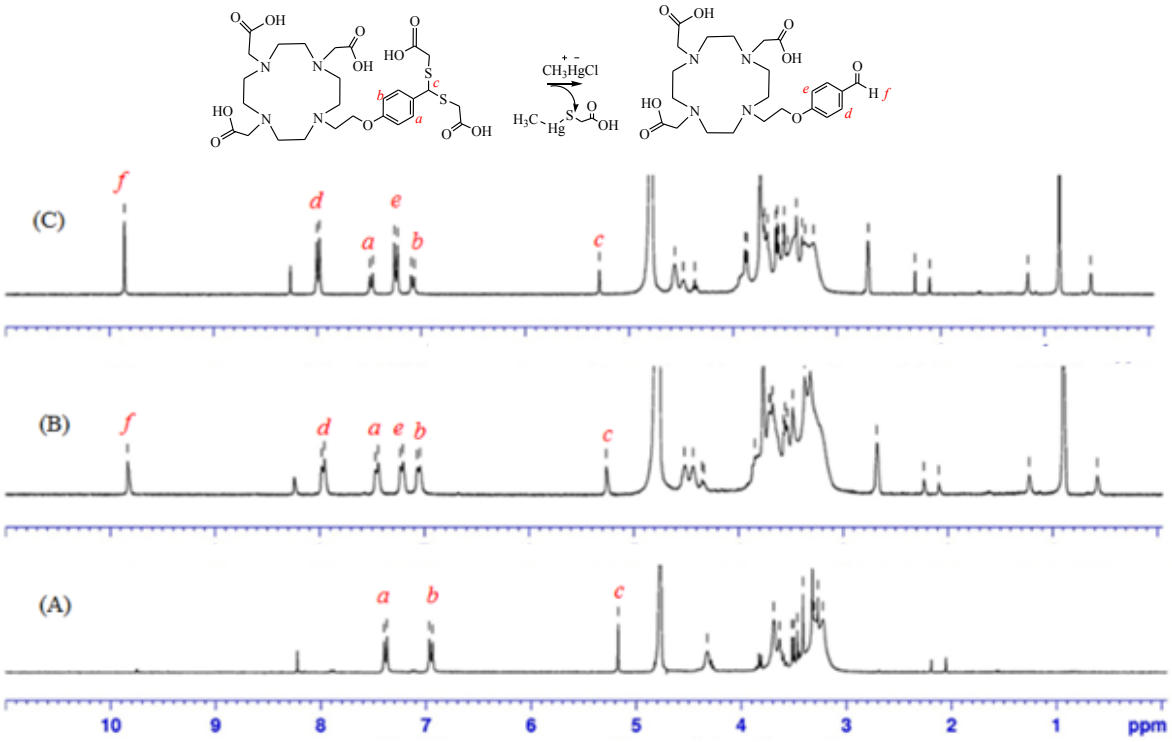

Fig. S2 ^{1}H NMR spectra (D_2O, 300 MHz): (A) *p*-MeHgGad ligand; (B) 1:1 mixture of *p*-MeHgGad ligand and CH_3Hg^+; (C) 1:2 mixture of *p*-MeHgGad ligand and CH_3Hg^+.

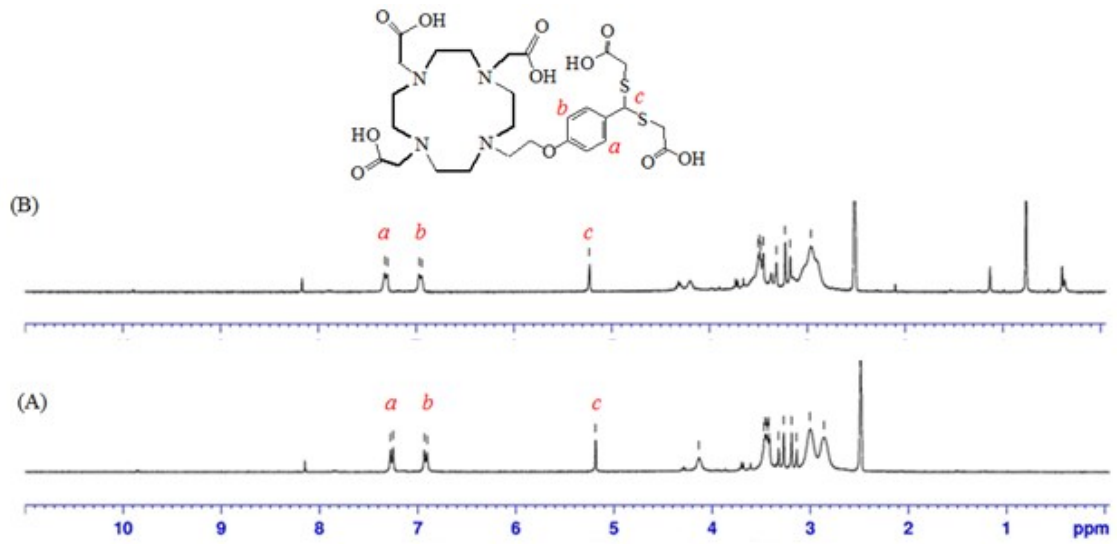

Fig. S3 ^{1}H NMR spectra (dry DMSO-d_6, 300 MHz): (A) *p*-MeHgGad ligand; (B) 1:3 mixture of *p*-MeHgGad ligand and CH_3Hg^+.

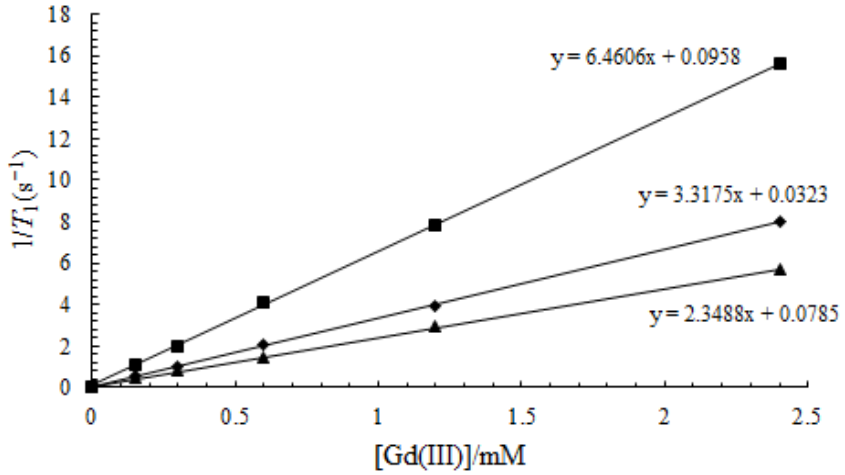

Fig. S4 Relaxivity of *p*-MeHgGad (■), DOTAREM® (♦), and *o*-MeHgGad (▲). All measurements were performed in 20mM HEPES buffer (pH 7.4) at 37.0 ± 0.1 ºC and 20 MHz. Gd(III) concentrations were determined by ICP-MS.

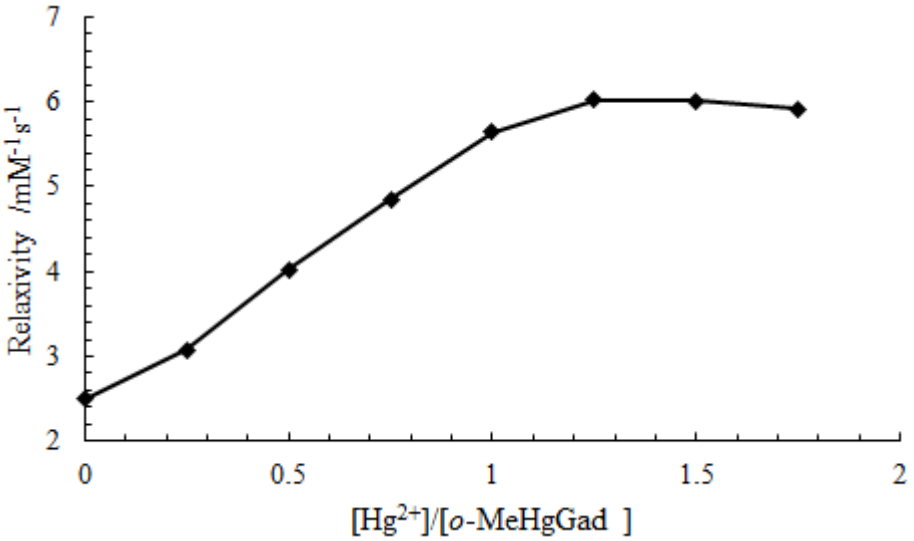

Fig. S5 Relaxivity response of *o*-MeHgGad (0.6 mM) to various concentration of Hg^{2+} ion at 37.0 ± 0.1 ºC and 20 MHz in 20 mM HEPES buffer pH 7.4.

^{1}H NMR, ^{13}C NMR, and HR-ESI spectra

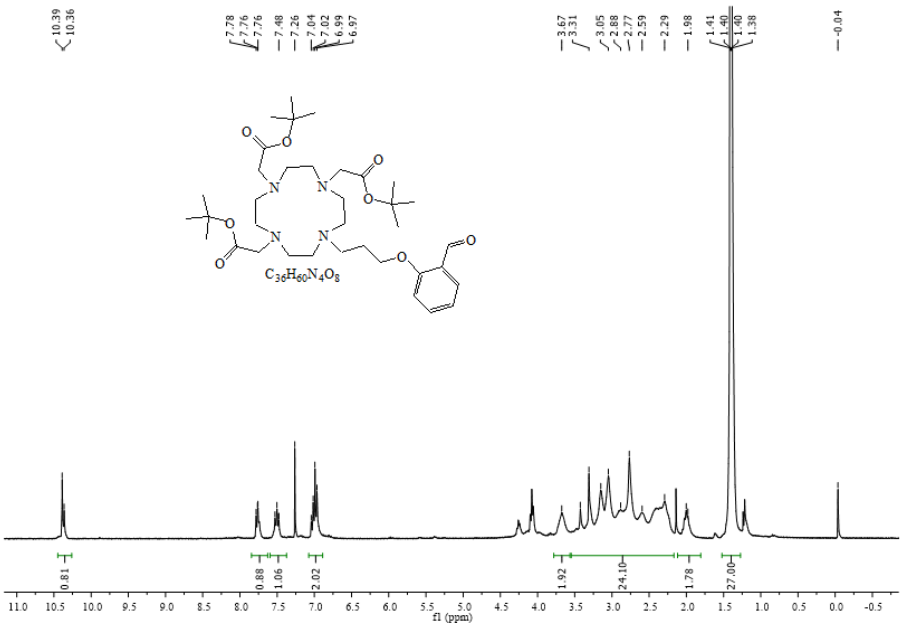

Fig.S6 ^{1}H NMR spectrum of tri-*tert*-butyl 2,2',2"-(10-(3-(2-formylphenoxy)propyl)-1,4,7,10-tetraazacyclododecane-1,4,7-triyl)triacetate (2)

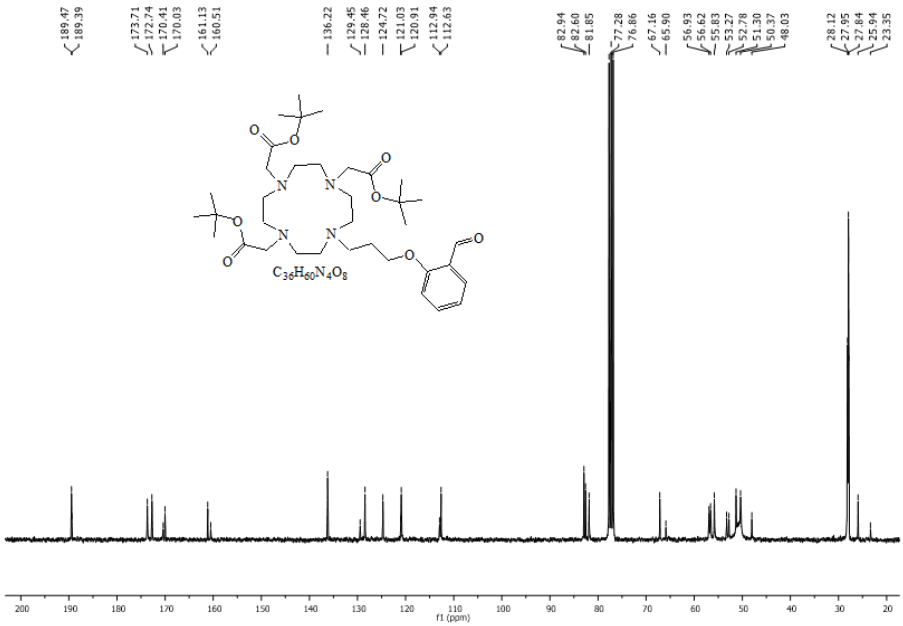

Fig. S7 ^{13}C NMR spectrum of tri-*tert*-butyl 2,2',2"-(10-(3-(2-formylphenoxy)propyl)-1,4,7,10-tetraazacyclododecane-1,4,7-triyl)triacetate (2)

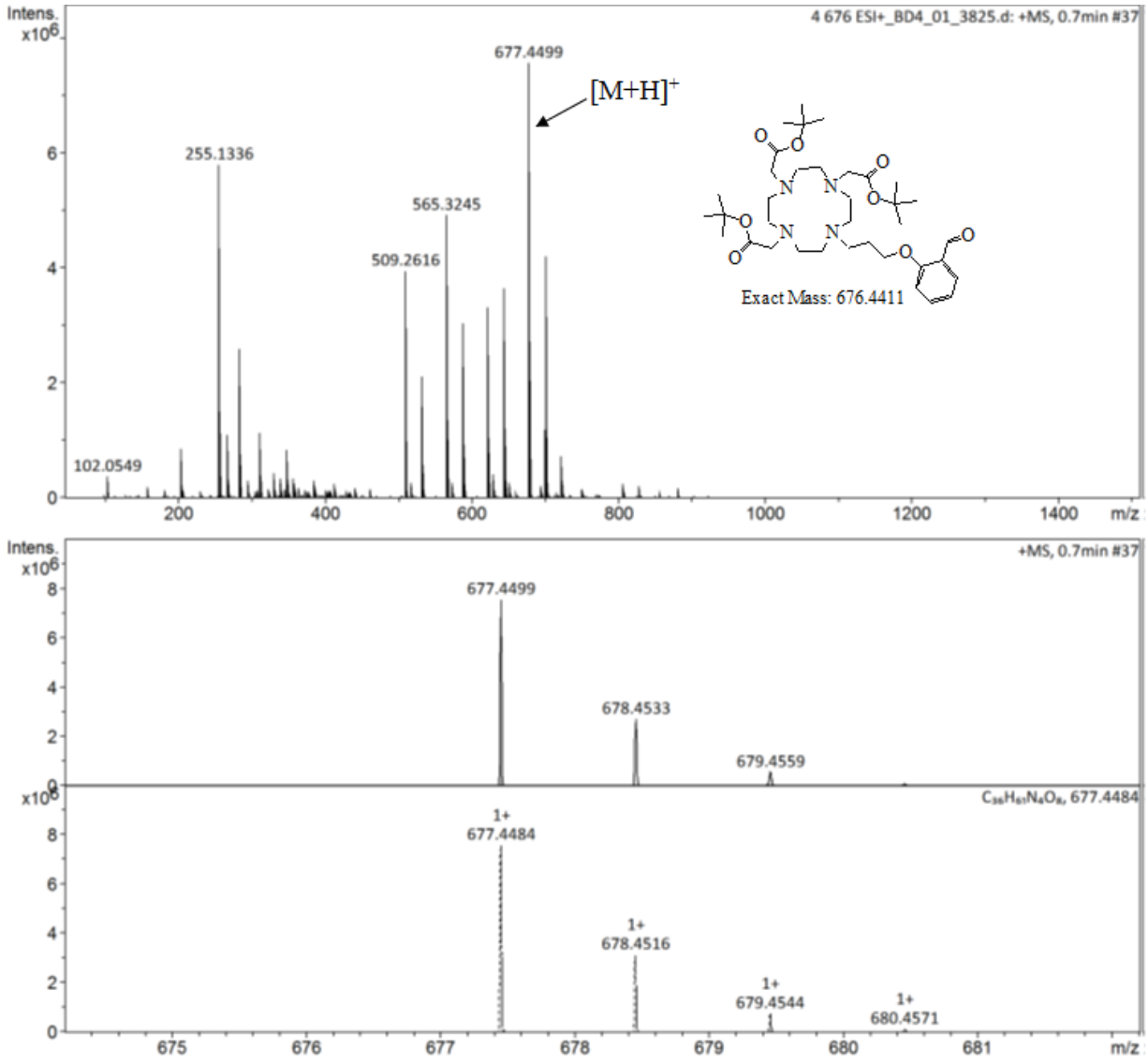

Fig. S8 HRESI-MS(ESI$^+$) spectrum of tri-*tert*-butyl 2,2',2''-(10-(3-(2-formylphenoxy)propyl)-1,4,7,10-tetraazacyclododecane-1,4,7-triyl)triacetate (2)

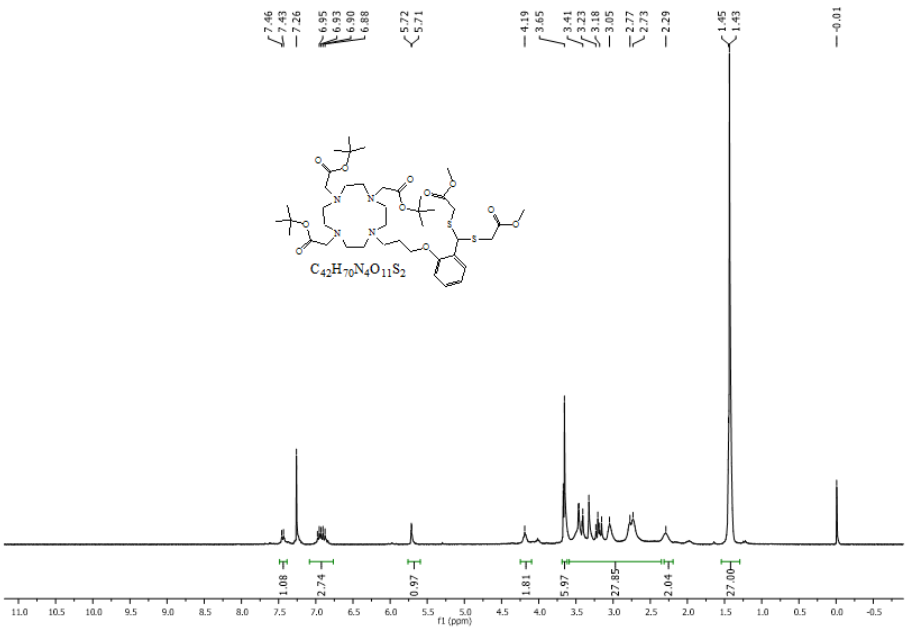

Fig. S9 ^{1}H NMR spectrum of tri-*tert*-butyl 2,2',2''-(10-(3-(2-(3,9-dioxo-2,10-dioxa-5,7-dithiaundecan-6 -yl)phenoxy)propyl)-1,4,7,10-tetraazacyclododecane-1,4,7-triyl)triacetate (3)

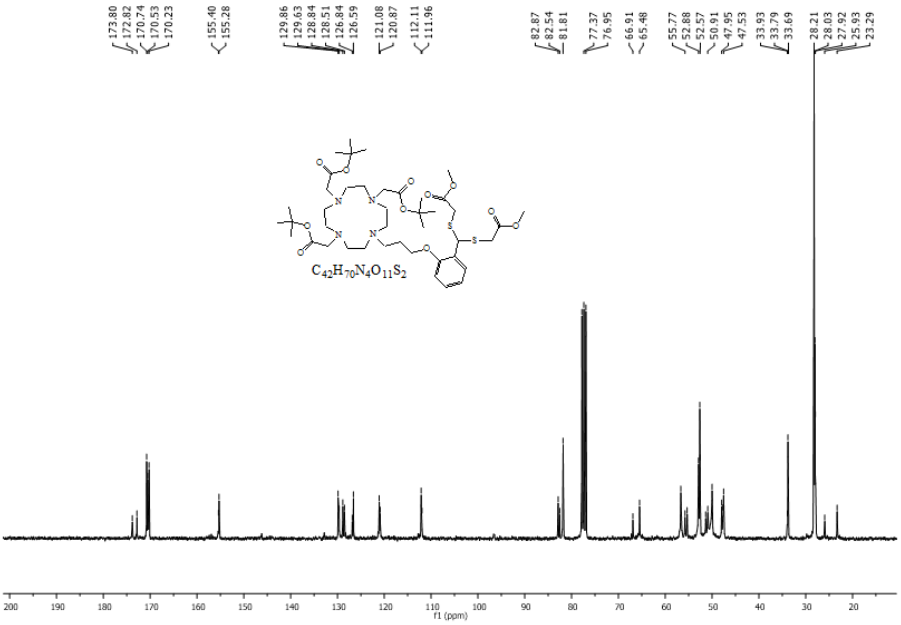

Fig. S10 ^{13}C NMR spectrum of tri-*tert*-butyl 2,2',2''-(10-(3-(2-(3,9-dioxo-2,10-dioxa-5,7-dithiaundecan-6 -yl)phenoxy)propyl)-1,4,7,10-tetraazacyclododecane-1,4,7-triyl)triacetate (3)

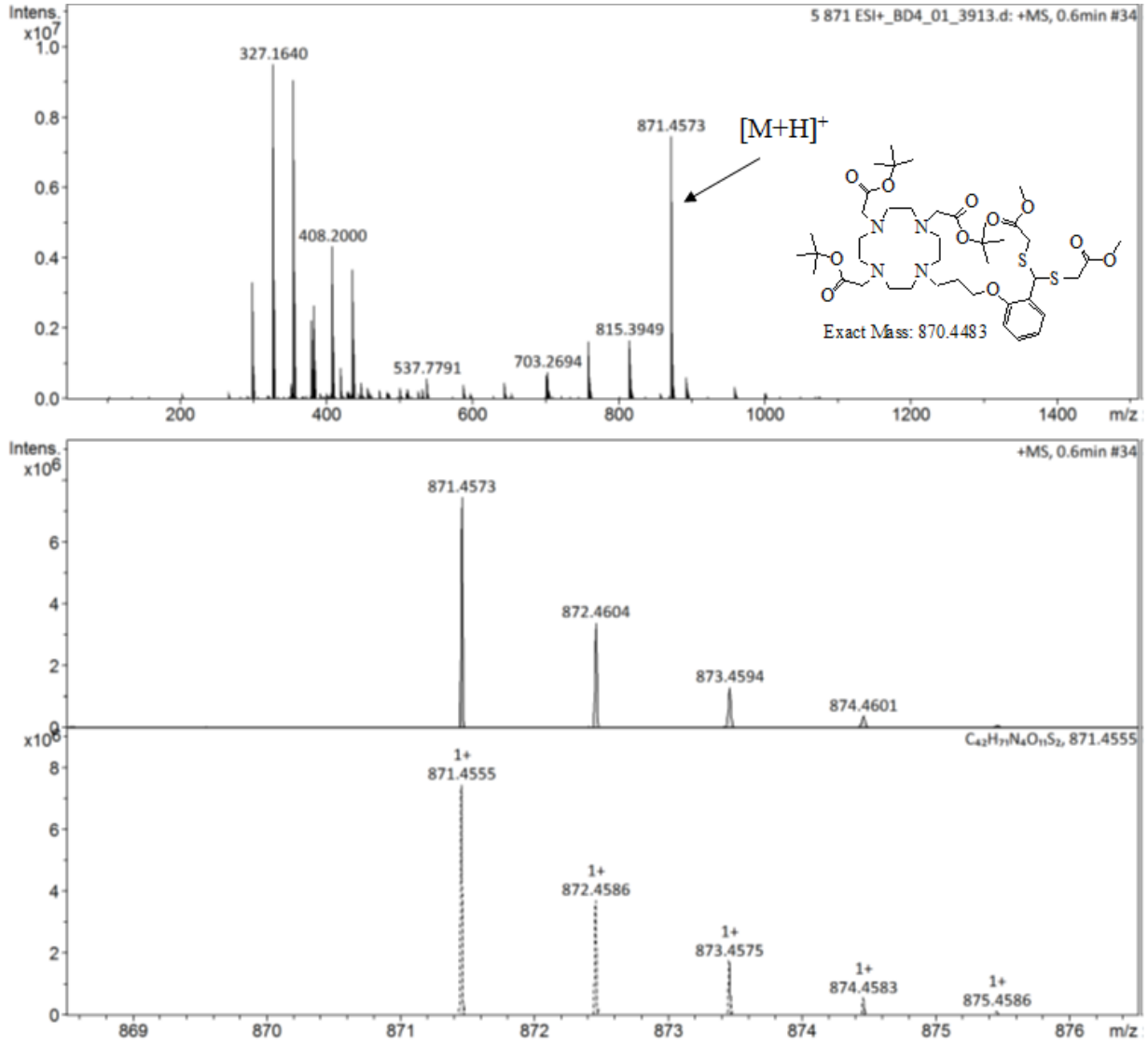

Fig. S11 HRESI-MS(ESI$^+$) spectrum of tri-*tert*-butyl 2,2',2''-(10-(3-(2-(3,9-dioxo-2,10-dioxa-5,7-dithiaundecan-6 -yl)phenoxy)propyl)-1,4,7,10-tetraazacyclododecane-1,4,7-triyl)triacetate (3)

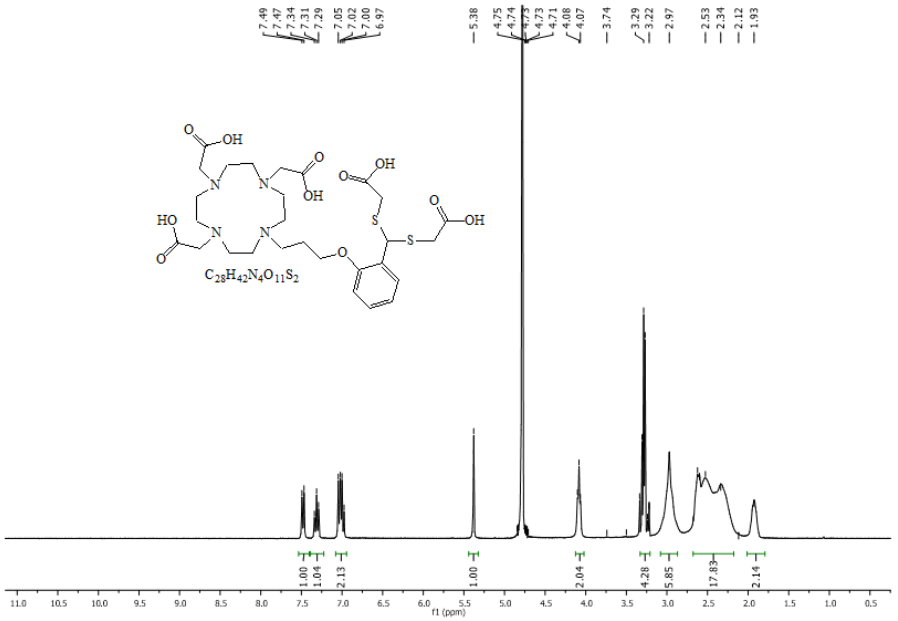

Fig. S12 ^{1}H NMR spectrum of 2,2',2''-(10-(3-(2 (bis((carboxymethyl) thio) methyl) phenoxy) propyl)-1,4,7,10-tetraazacyclododecane-1,4,7-triyl)triacetic acid (4)

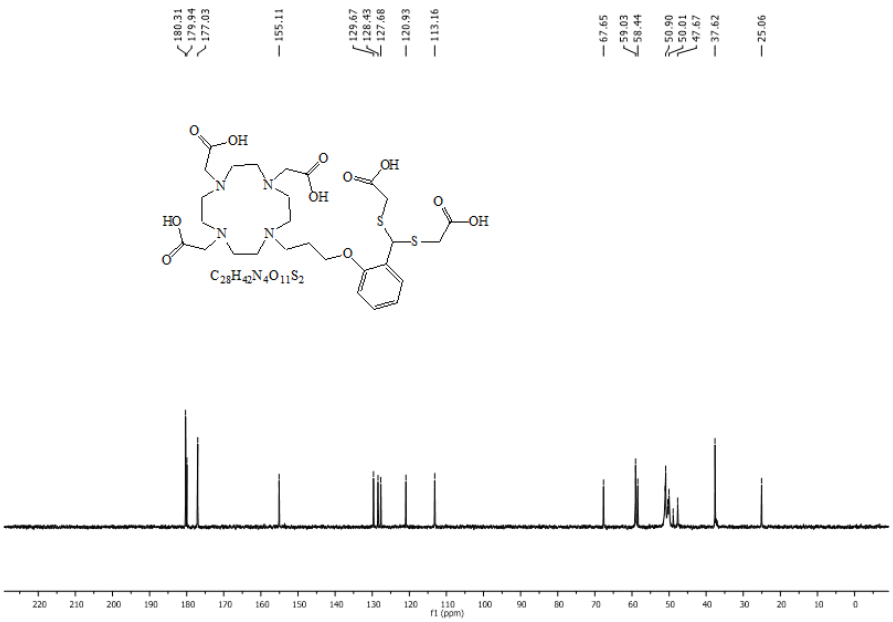

Fig. S13 ^{13}C NMR spectrum of 2,2',2''-(10-(3-(2 (bis((carboxymethyl) thio)methyl) phenoxy) propyl)-1,4,7,10-tetraazacyclododecane-1,4,7-triyl)triacetic acid (4)

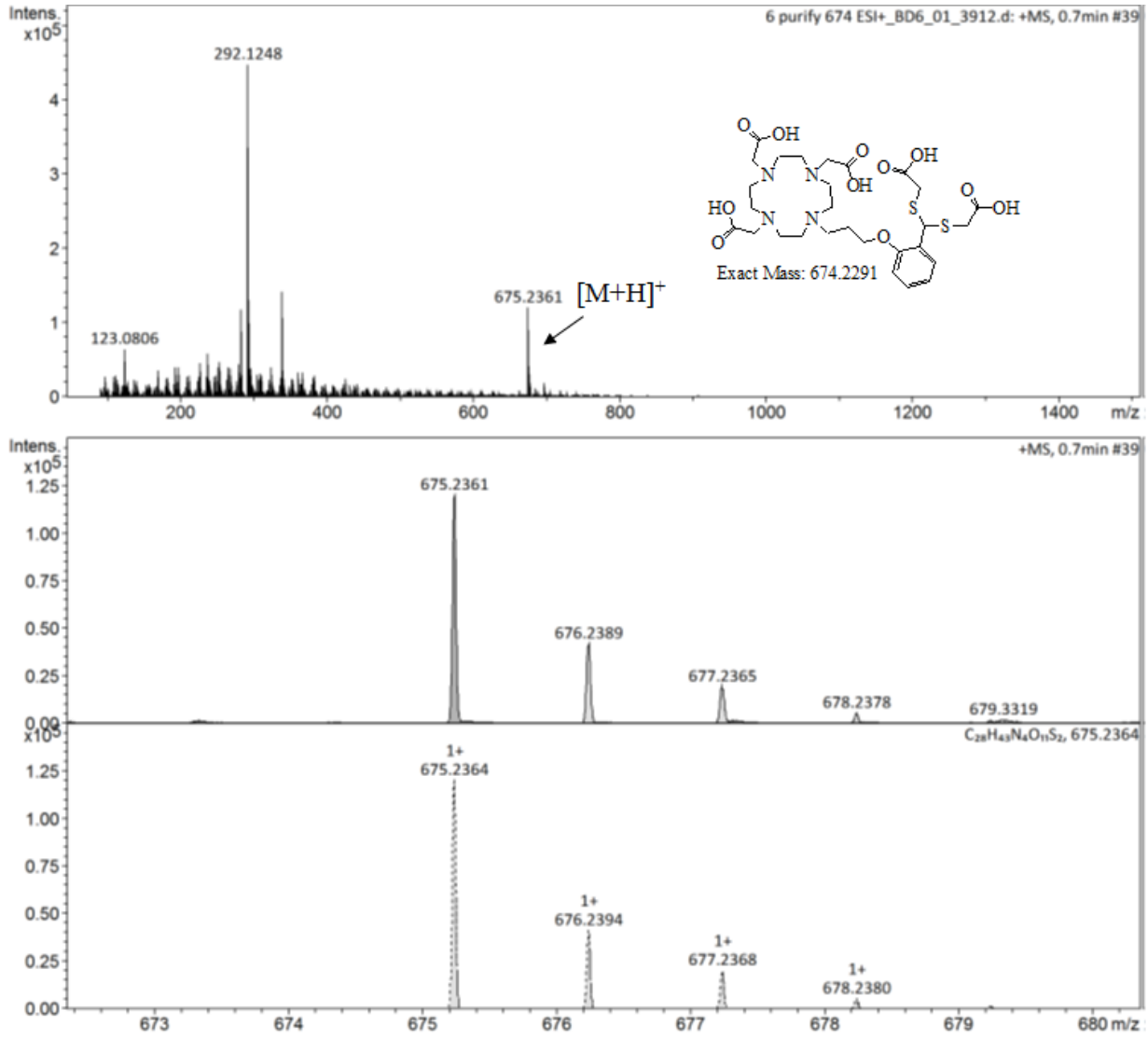

Fig. S14 HRESI-MS(ESI$^+$) spectrum of 2,2',2''-(10-(3-(2 (bis((carboxymethyl) thio)methyl) phenoxy)propyl)-1,4,7,10-tetraazacyclododecane-1,4,7-triyl)triacetic acid (4)

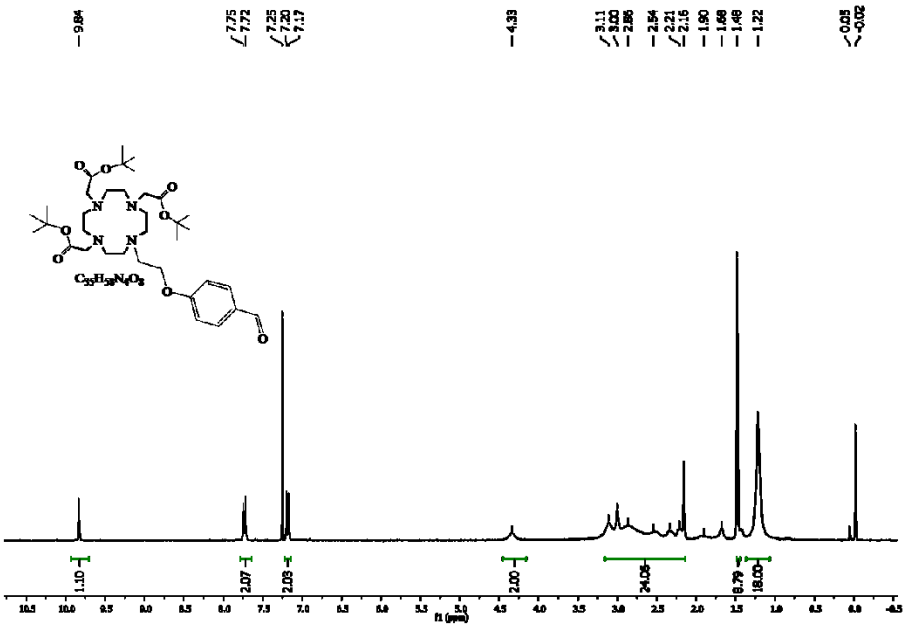

Fig. S15 ^{1}H NMR spectrum of tri-*tert*-butyl 2,2',2''-(10-(2-(4-formylphenoxy)ethyl)-1,4,7,10-tetraazacyclododecane-1,4,7-triyl)triacetate (2a)

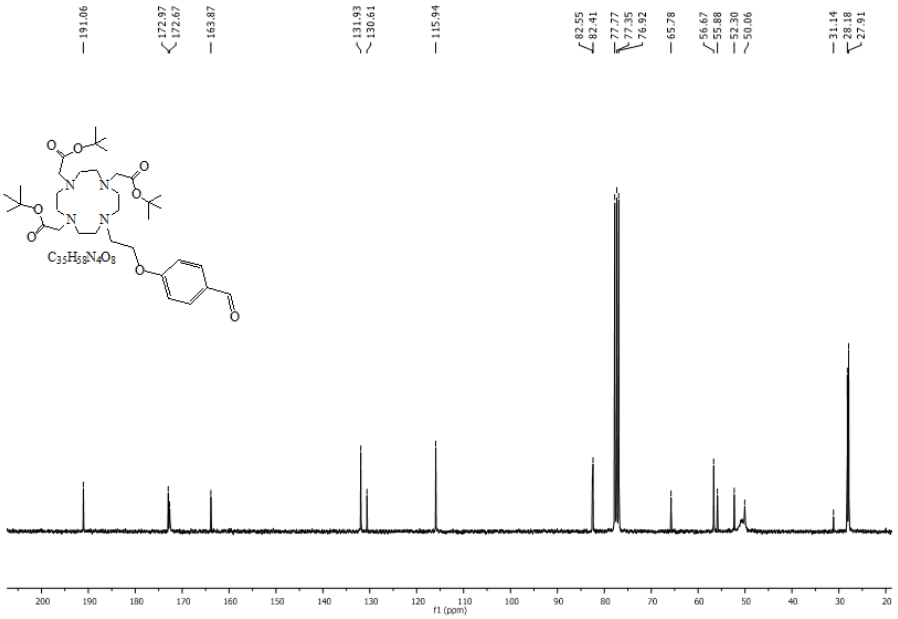

Fig. S16 ^{13}C NMR spectrum of tri-*tert*-butyl 2,2',2''-(10-(2-(4-formylphenoxy)ethyl)-1,4,7,10-tetraazacyclododecane-1,4,7-triyl)triacetate (2a)

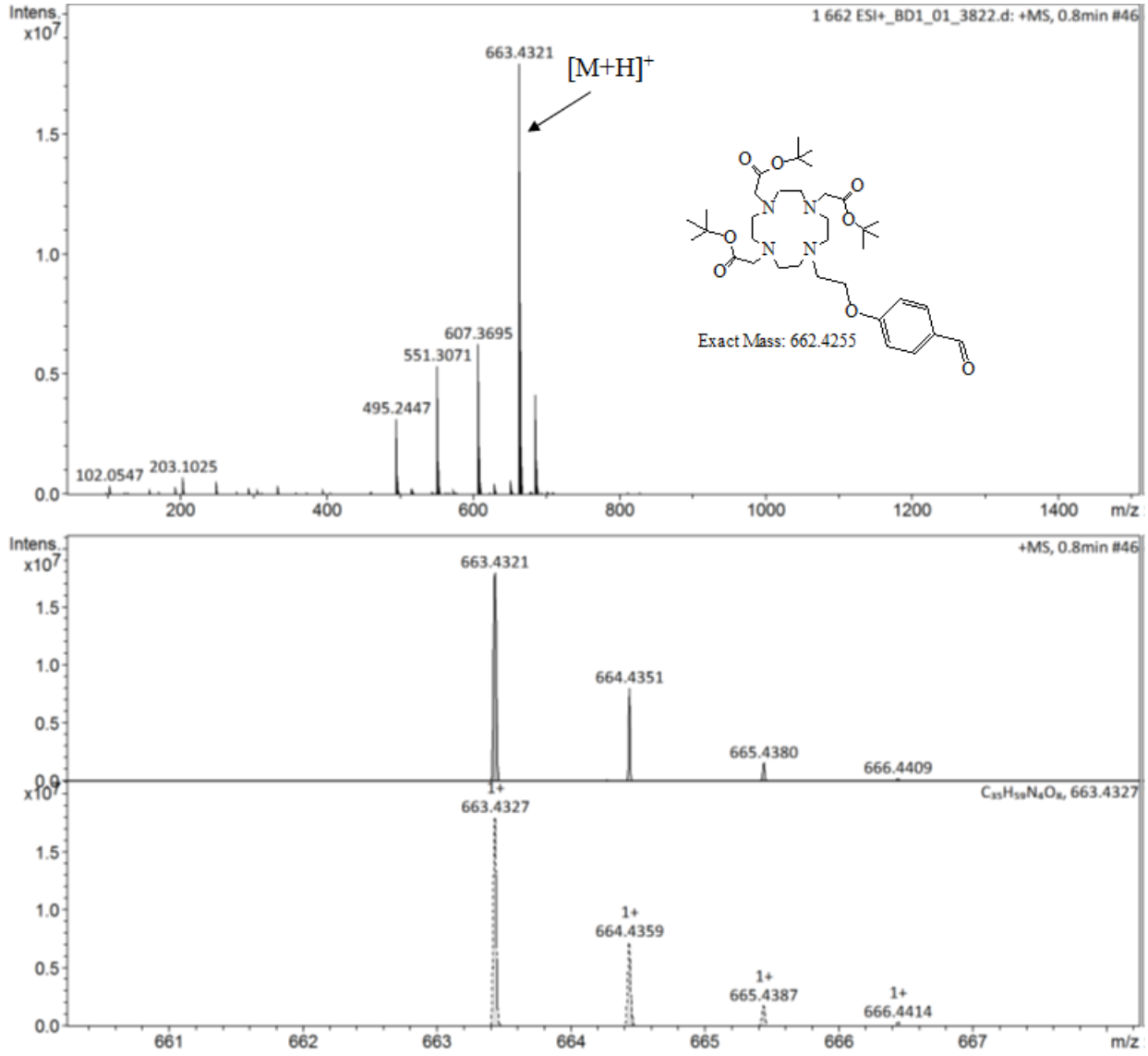

Fig. S17 HRESI-MS(ESI$^+$) spectrum of tri-*tert*-butyl 2,2',2''-(10-(2-(4-formylphenoxy)ethyl)-1,4,7,10-tetraazacyclododecane-1,4,7-triyl)triacetate (2a)

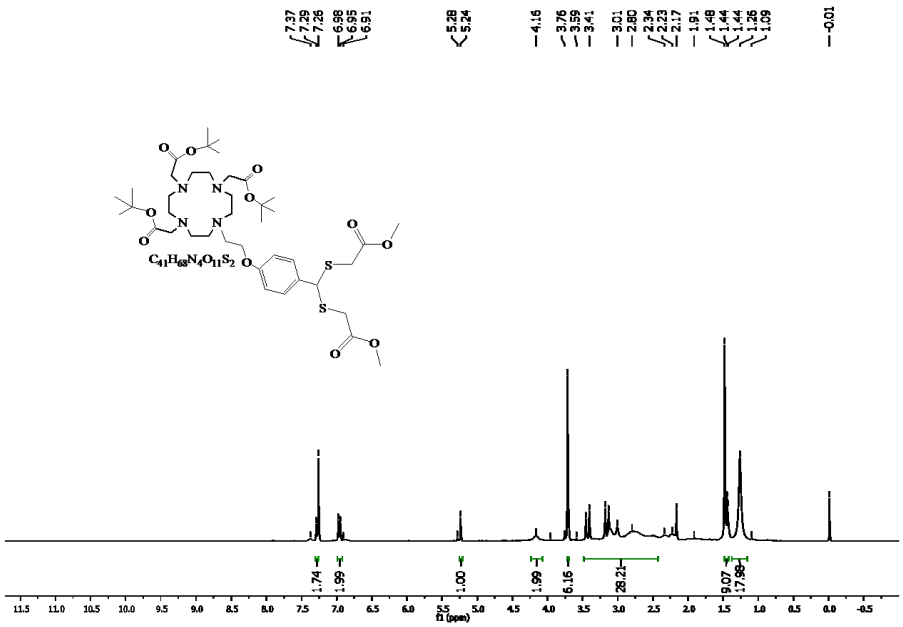

Fig. S18 ^{1}H NMR spectrum of tri-*tert*-butyl 2,2',2''-(10-(2-(4-(3,9-dioxo-2,10-dioxa-5,7-dithiaundecan-6-yl)phenoxy)ethyl)-1,4,7,10-tetraazacyclododecane-1,4,7-triyl)triacetate (3a)

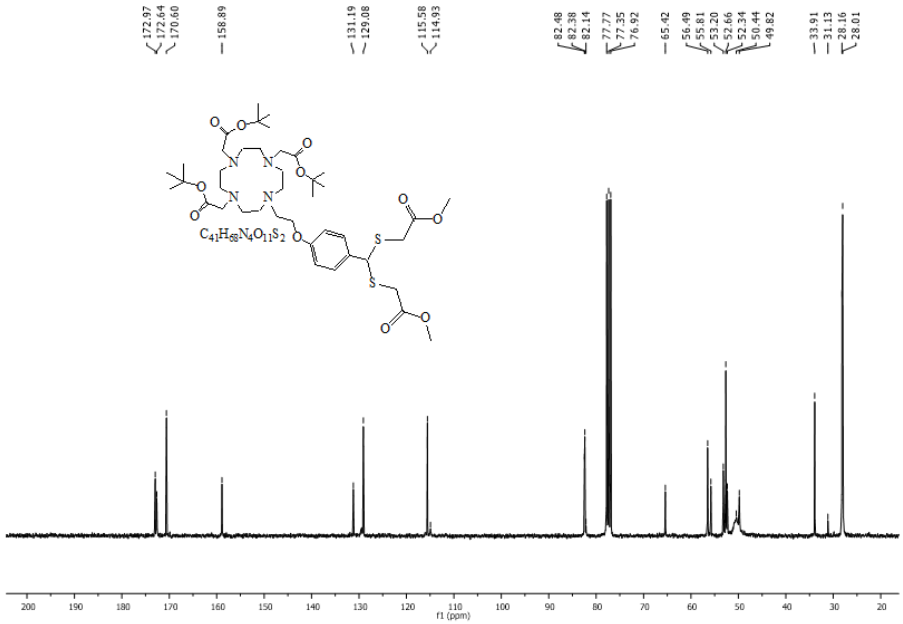

Fig. S19 ^{13}C NMR spectrum of tri-*tert*-butyl 2,2',2''-(10-(2-(4-(3,9-dioxo-2,10-dioxa-5,7-dithiaundecan-6-yl)phenoxy)ethyl)-1,4,7,10-tetraazacyclododecane-1,4,7-triyl)triacetate (3a)

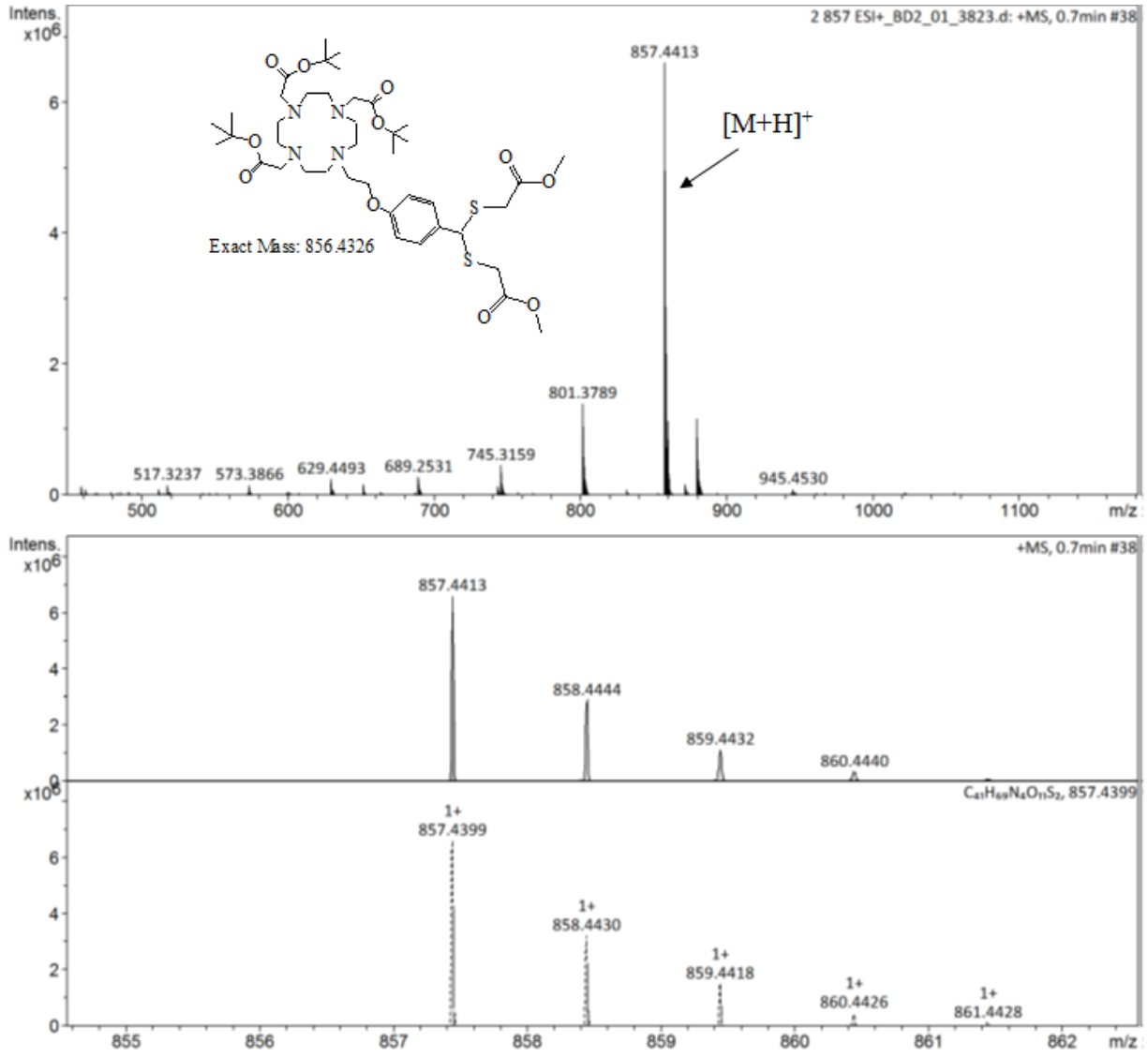

Fig. S20 HRESI-MS(ESI$^+$) spectrum of tri-*tert*-butyl 2,2',2''-(10-(2-(4-(3,9-dioxo-2,10-dioxa-5,7-dithiaundecan-6-yl)phenoxy)ethyl)-1,4,7,10-tetraazacyclododecane-1,4,7-triyl)triacetate (3a)

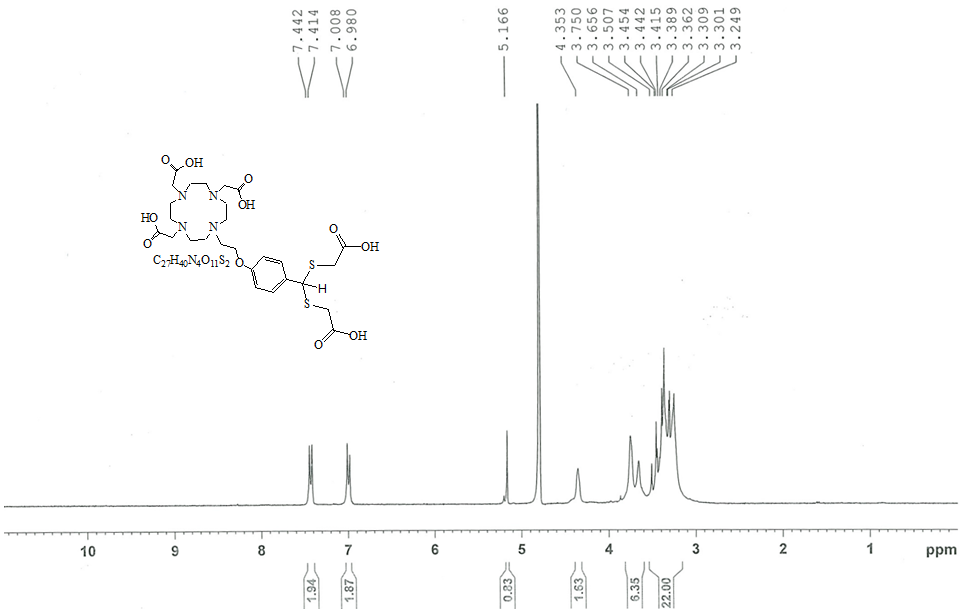

Fig. S21 ^{1}H NMR spectrum of 2,2',2''-(10-(2-(4-(bis((carboxymethyl) thio)methyl)phenoxy) ethyl)-1,4,7,10-tetraazacyclododecane-1,4,7-triyl)triacetic acid (4a)

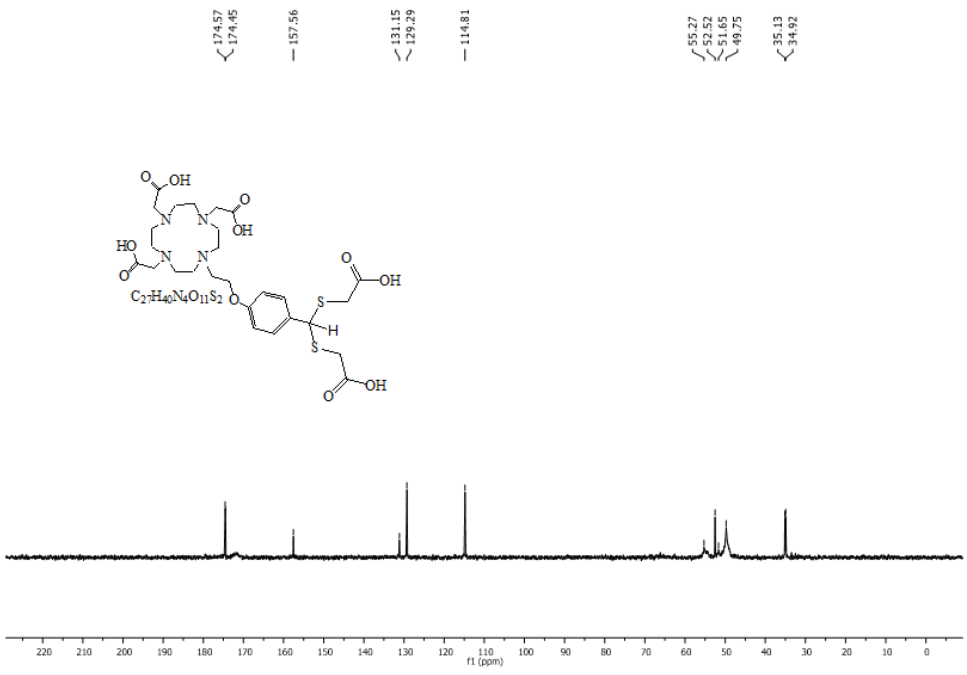

Fig. S22 ^{13}C NMR spectrum of 2,2',2''-(10-(2-(4-(bis((carboxymethyl)thio)methyl) phenoxy)ethyl)-1,4,7,10-tetraazacyclododecane-1,4,7-triyl)triacetic acid (4a)

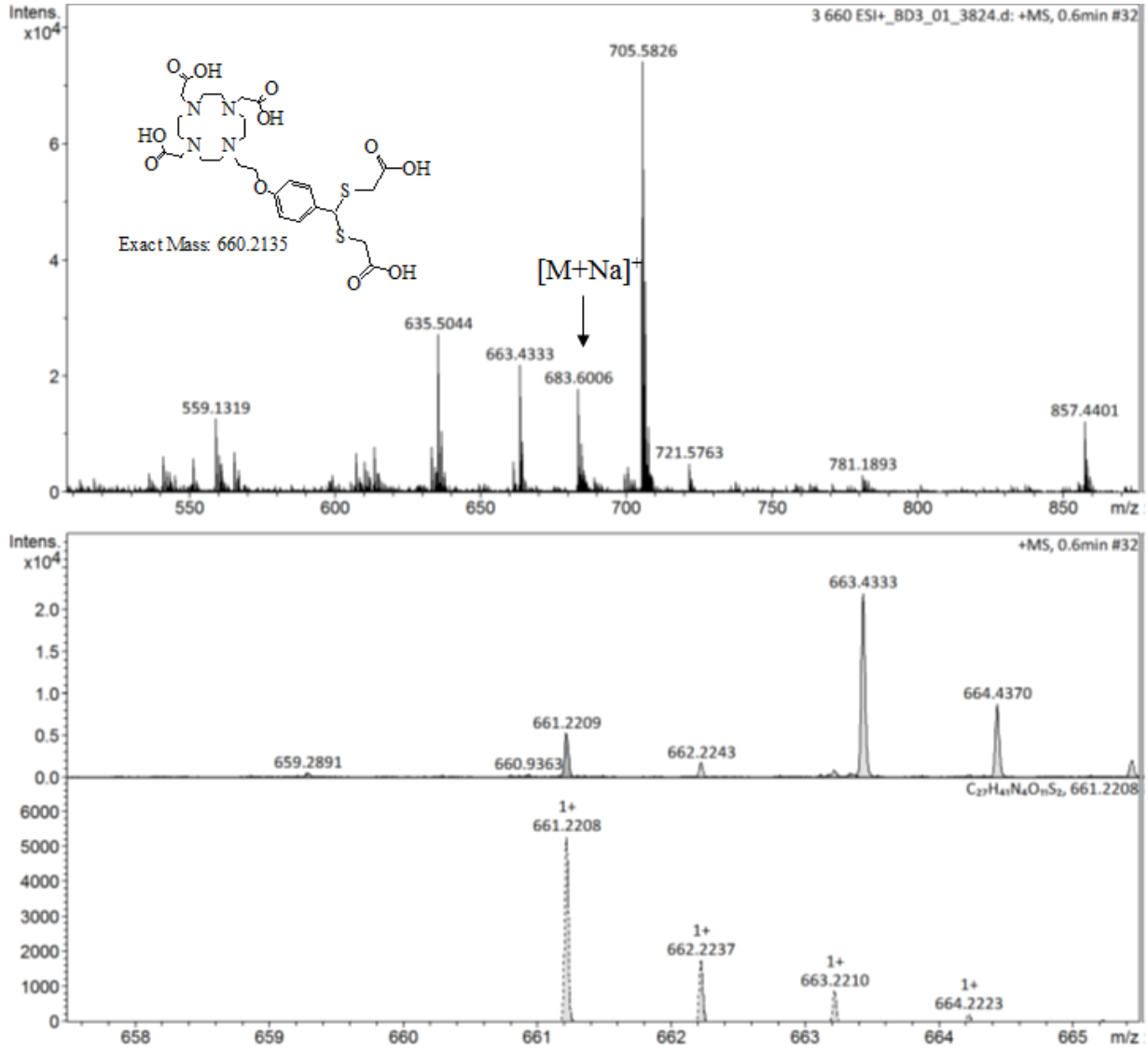

Fig. S23 HRESI-MS(ESI$^+$) spectrum of 2,2',2''-(10-(2-(4-(bis((carboxymethyl)thio)methyl) phenoxy)ethyl)-1,4,7,10-tetraazacyclododecane-1,4,7-triyl)triacetic acid (4a)

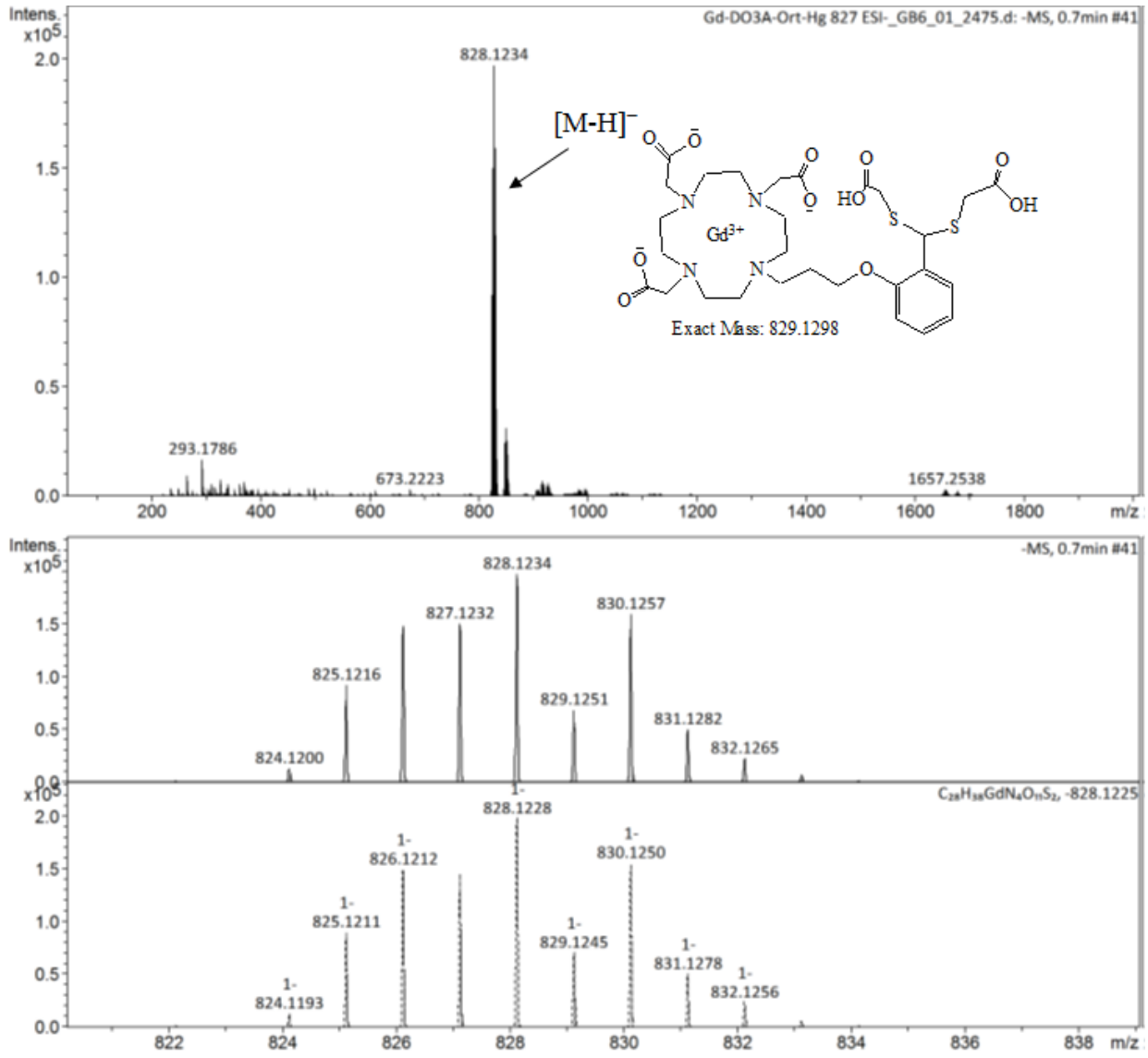

Fig. S24 HRESI-MS (ESI⁻) spectrum of *o*-MeHgGad

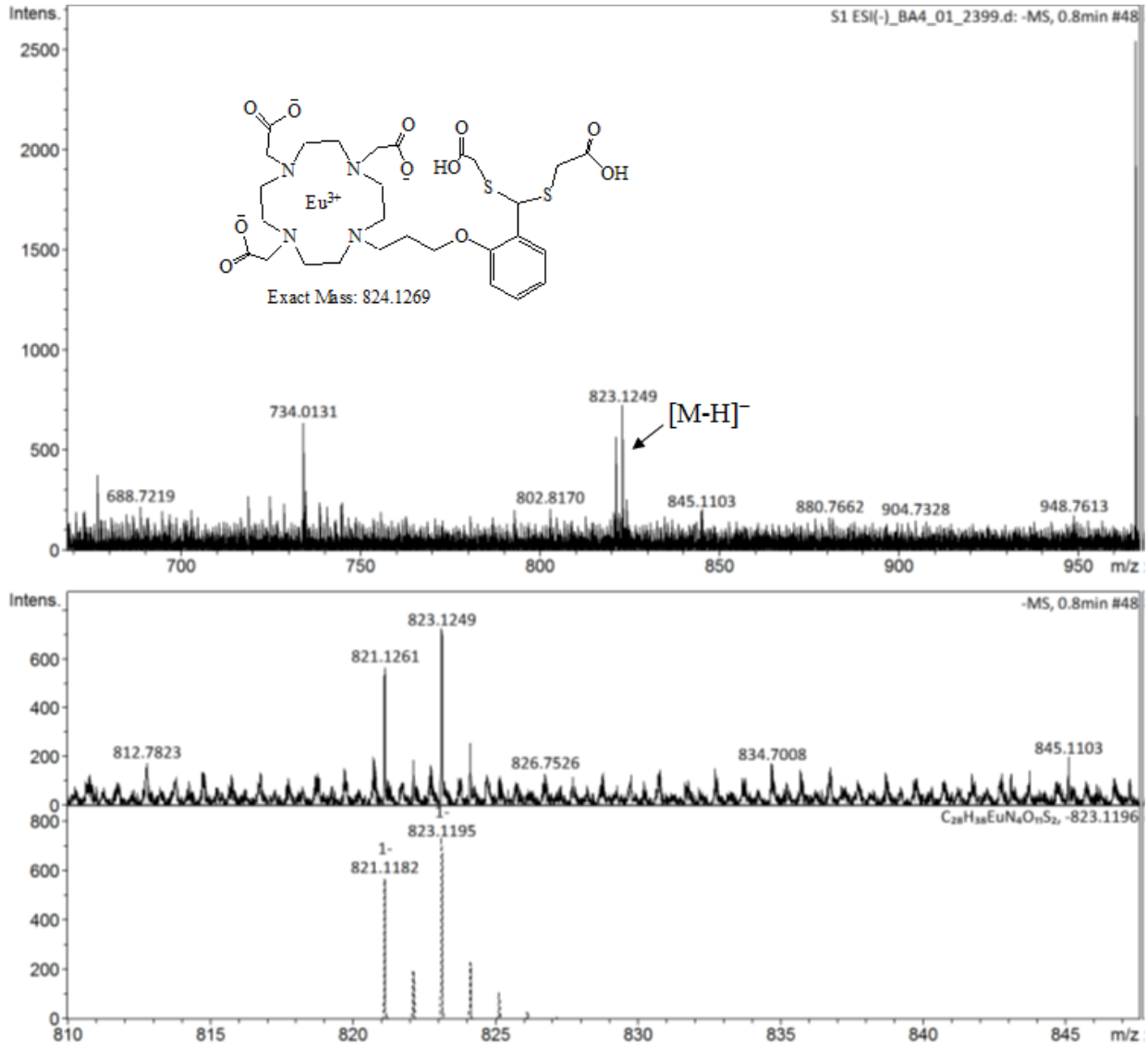

Fig. S25 HRESI-MS (ESI⁻) spectrum of *o*-MeHgEur

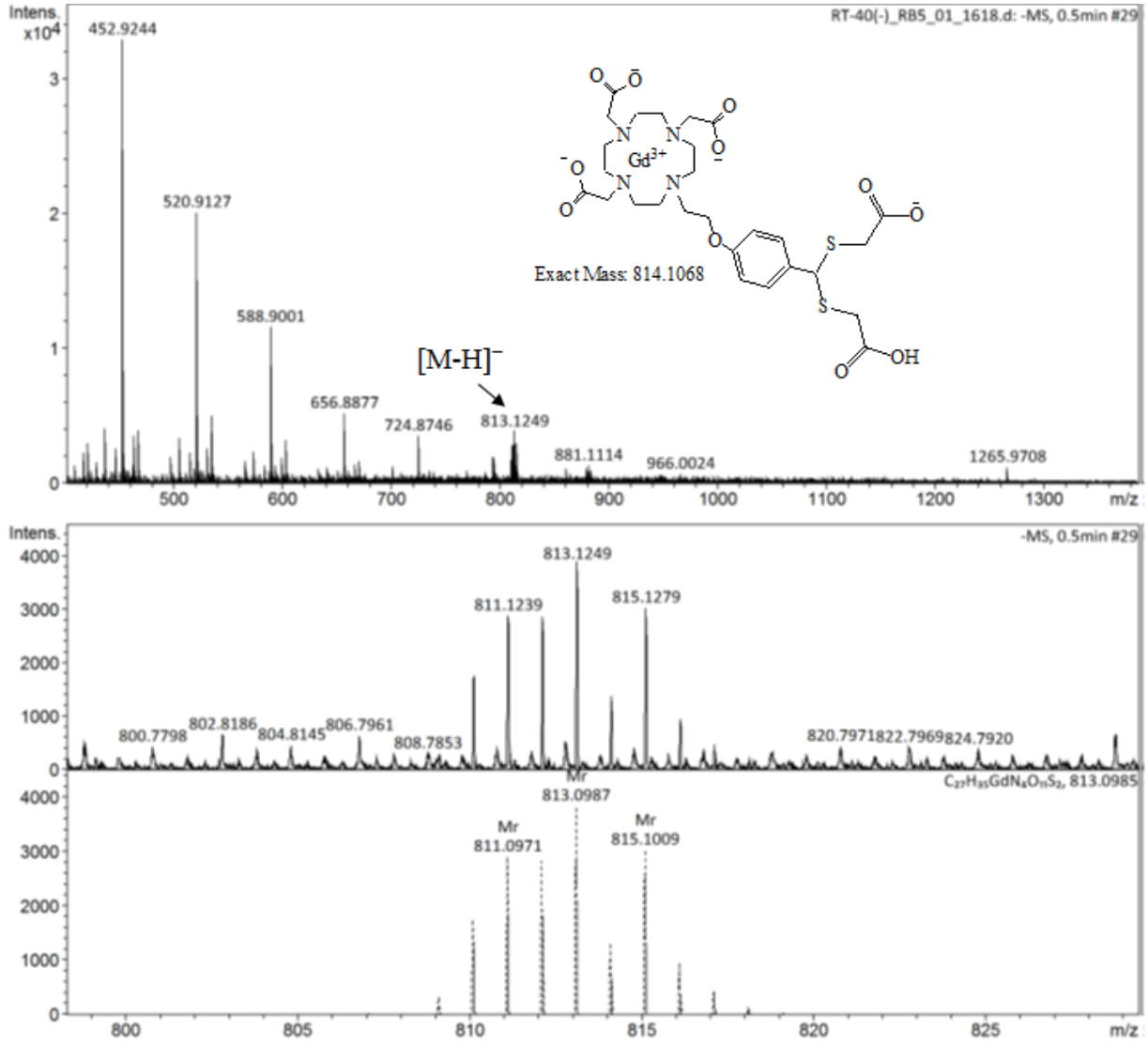

Fig. S26 HRESI-MS (ESI⁻) spectrum of *p*-MeHgGad

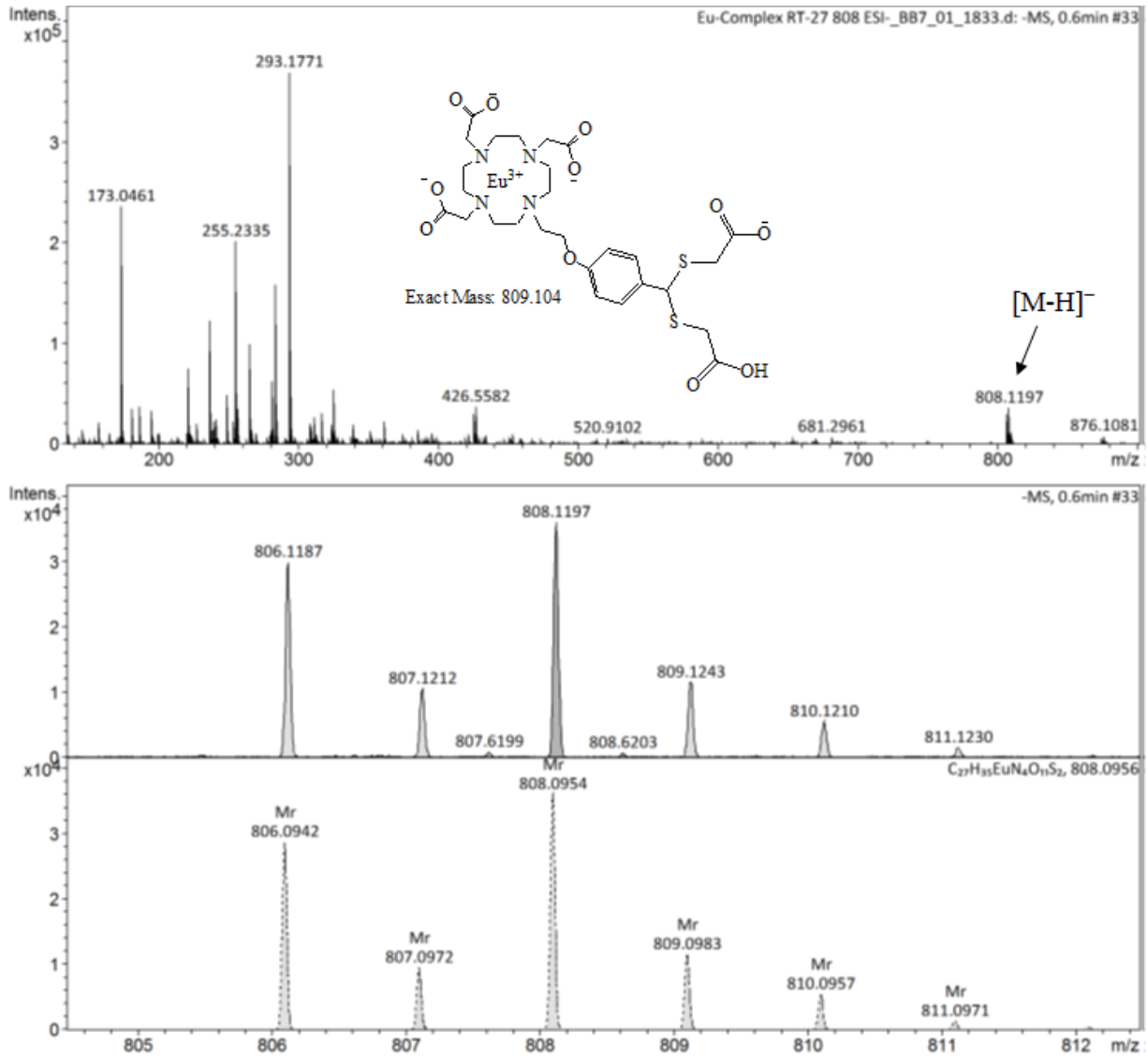

Fig. S27 HRESI-MS (ESI⁻) spectrum of *p*-MeHgEur

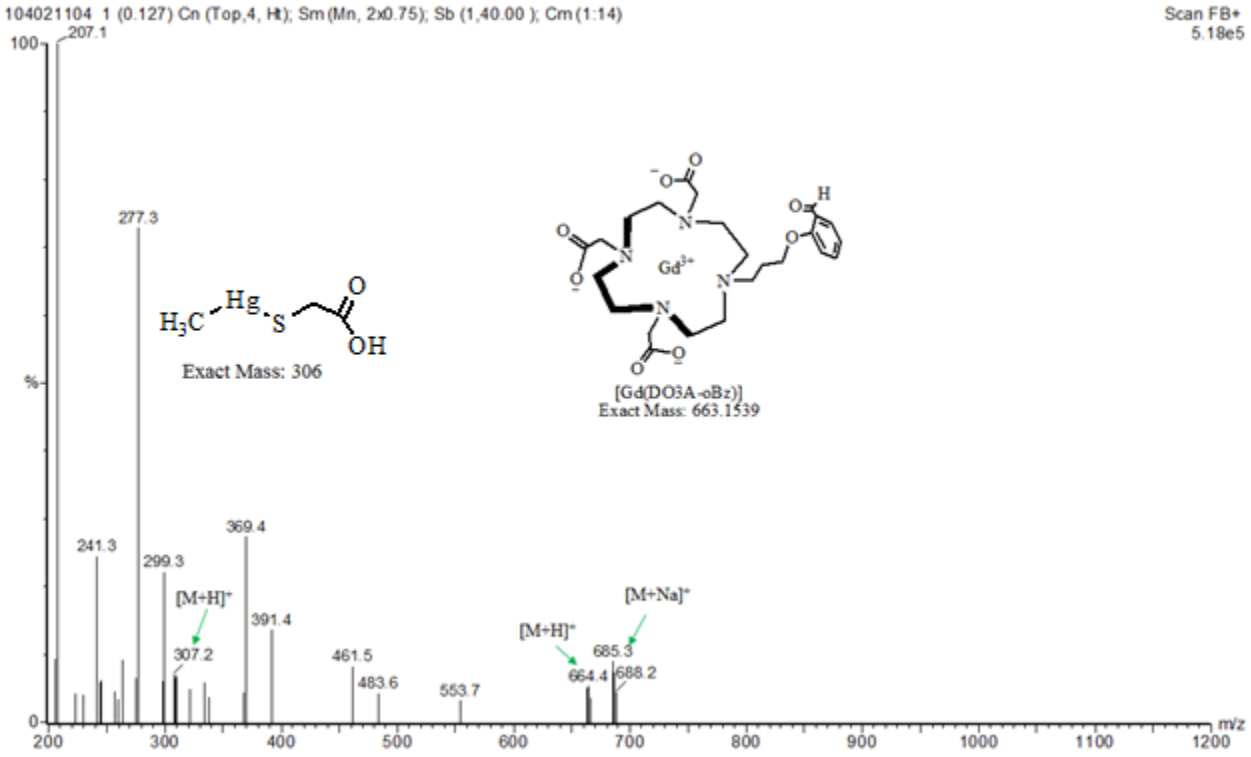

Fig. S28 FAB (+) spectrum of *o*-MeHgGad in the presence of 2 equiv. CH_3Hg^+

1 S. Mizukami, R. Takikawa, F. Sugihara, Y. Hori, H. Tochio, M. Wälchli, M. Shirakawa and K. Kikuchi, *J. Am. Chem. Soc.* 2008,**130**, 794-795

2 A. Khalafi-Nezhad, M. Divar and F. Panahi, *J. Org. Chem.* 2013**, 78**, 10902-10908

3 (a) A. Beeby, I. M. Clarkson, R. S. Dickins, S. Faulkner, D. Parker, L. Royle, A. S. d. Sousa, J. A. G. Williams and M. Woods, *J. Chem. Soc., Perkin Trans. 2*, 1999, 493; (b) W. D. Horrocks and D. R. Sudnick, *J. Am. Chem. Soc.* 1979, **101**, 334.